

MASTER

CONF-771035-8
TITLE: RELATIVISTIC ELECTRON BEAM CYCLOTRON WAVE
GROWTH IN HELICAL SLOW WAVE STRUCTURES*

AUTHOR(S): B. B. Godfrey, R. J. Faehl, B. S. Newberger,
W. R. Shanahan, and L. E. Thode

SUBMITTED TO: 2nd International Topical Conference
on High Power Electron and Ion Beam
Research and Technology

NOTICE
This report was prepared as an account of work sponsored by the United States Government. Neither the United States nor the United States Energy Research and Development Administration, nor any of their employees, nor any of their contractors, subcontractors, or their employees, makes any warranty, express or implied, or assumes any legal liability or responsibility for the accuracy, completeness or usefulness of any information, apparatus, product or process disclosed, or represents that its use would not infringe privately owned rights.

By acceptance of this article for publication, the publisher recognizes the Government's (license) rights in any copyright and the Government and its authorized representatives have unrestricted right to reproduce in whole or in part said article under any copyright secured by the publisher.

The Los Alamos Scientific Laboratory requests that the publisher identify this article as work performed under the auspices of the USERDA.



An Affirmative Action/Equal Opportunity Employer

DISTRIBUTION OF THIS DOCUMENT IS UNLIMITED

RELATIVISTIC ELECTRON BEAM CYCLOTRON WAVE GROWTH
IN HELICAL SLOW WAVE STRUCTURES*

B. B. Godfrey, R. J. Faehl, B. S. Newberger,
W. R. Shanahan, and L. E. Thode
Theoretical Division, Los Alamos Scientific Laboratory
Los Alamos, New Mexico 87545

One of the more promising and thoroughly studied proposals for high energy collective ion acceleration is Autoresonant Acceleration: Ions trapped in the electrostatic wells of large amplitude slow cyclotron waves in an unneutralized intense relativistic electron beam are accelerated by the increase of wave phase velocity as the beam propagates along a magnetic guide field of decreasing strength. A critical component of this scheme is growth of coherent, large amplitude waves. Here, we consider wave growth by interaction of the beam with a helical slow wave structure. Specific topics include (1) equilibrium charge and current distributions on the helix, (2) linear wave growth spectra including the effects of radial inhomogeneity, (3) wave growth and saturation, and (4) extraction of cyclotron waves from the amplifier cavity. Movies of two-dimensional computer simulations are presented. We find that waves of amplitude adequate for planned feasibility experiments can indeed be obtained.

I. INTRODUCTION

Collective ion acceleration is a highly speculative, yet potentially very significant, application for intense relativistic electron beams. Eventually, it may permit the compact and economical acceleration of substantial currents of light or heavy ions to hundreds of MeV per nucleon. All collective

acceleration schemes presently envisioned involve three key stages. Slowly moving large amplitude electrostatic potential wells are established in an intense relativistic electron beam, an adequate number of ions are trapped in those wells, and the wells with trapped ions are smoothly accelerated to velocities approaching that of the beam. Obvious sources for such potential wells are the large charge gradient at the head of an electron beam and large amplitude Langmuir or cyclotron waves in the body of the beam.¹

One of the more promising and thoroughly studied high energy collective ion acceleration schemes is the Autoresonant Acceleration proposal by Sloan and Drummond.² It employs the slow cyclotron wave in an unneutralized intense relativistic electron beam propagating in vacuum along a strong axial magnetic field. Control of the wave phase velocity is achieved through spatial variation of the guide magnetic field. Austin Research Associates, Inc. is soon to begin an experimental investigation of this concept.³ A 30 kA, 3 MeV, 200 ns electron beam will be used. Present plans call for the cyclotron waves to be grown in a slow wave structure at 3.4 kg. The beam is then adiabatically compressed in a field increasing to 25 kg, and ions loaded. Subsequent decrease of the axial field to 2.5 kg in the acceleration section should yield 30 MeV ions.

For a successful experiment, the wave growth section must produce reasonably monochromatic, large amplitude, axially symmetric slow cyclotron waves while avoiding competing, disruptive instabilities. We at Los Alamos Scientific Laboratory are studying both analytically and computationally wave

amplification in a sheath helix slow wave structure, one of two active candidates for the planned experiment. Our results, although not yet complete, are encouraging.

Section II describes the problem of establishing equilibrium between the beam and the helix. This is important, because the helix, being both capacitive and inductive, can support large transients lasting throughout the beam pulse. We show, however, that a proper combination of resistive termination of the helix and shaping of the beam pulse reduces transients to an innocuous level. Return currents in the helix, which disrupt the externally applied magnetic guide field, probably can be treated in the same way.

Because the slow cyclotron wave is of negative energy, while the helix-supported wave is of positive energy, they interact to produce a moderately rapidly growing convective instability which is to be responsible for cyclotron wave amplification. Section III gives the linear theory of this instability, obtained numerically from GRADR, a dispersion relation solver for radially inhomogeneous, cylindrically symmetric, cold fluid beam equilibria.⁴ Analytic approximations are also provided.

Based on the linear theory, two-dimension computer simulations in cylindrical geometry have been performed with CCUBE.⁵ Simulations show that, for a 2.65 cm radius beam in a 15° pitch helix at 3.8 cm both enclosed in a metal waveguide at 5.7 cm, cyclotron waves grow from a fractional modulation of 1/2% to about 40% in just more than a meter distance. Growth stops only when the waves leave the helix or electrons actually strike the helix. Wave growth obeys linear theory well,

with little sign of nonlinear effects even at large amplitude. All this appears in Section IV.

Section V discusses extraction of the large amplitude cyclotron waves from the helical amplifier. To date, our investigation has been limited to comparison of the linearized eigenmodes in the helix and in a waveguide of equal radius. Although frequency and wavenumber are essentially unchanged, the radial profiles of the wave components are significantly modified. The impact of this mismatch remains to be seen.

II. BEAM-HELIX EQUILIBRIUM

Fig. 1 shows the relativistic electron beam just entering the helix. The small plus signs at the helix and outer conducting waveguide represent image charges induced by the beam. Placement of these plus signs is meant to illustrate a key feature of the early time beam-helix interaction. Image charges on the helix move at a velocity

$$v_H = \frac{c \sin \psi}{[1 - (1 + \frac{1-\alpha}{\ell n \alpha}) \cos^2 \psi]^{1/2}} , \quad (1)$$
$$\alpha \equiv (R_H/R_W)^2 < 1 ,$$

which for our purposes is somewhat less than the beam velocity, $v_B \approx c$. For example, with the parameters cited in the Introduction, $v_H \approx 0.3 c$. Therefore, even though both ends of the helix may be grounded, the head of the beam soon outruns image charges on the helix and sees the outer conductor as the ground plane. For the experimental beam parameters, space charge effects limit R_W to no greater than $2.4 R_B$ for a fast beam risetime. The 80 ns risetime contemplated in the Austin Research Associates, Inc. experiment will, of course, substantially weaken this constraint.

Of greater importance is the fact that, because the beam reaches the far end of the helix before helix image charges do, additional image charges begin flowing onto the helix. The two streams of image charge from each end do not interact when they meet near the center but simply flow on to the helix ends, where they reflect, and so continue to stream back and forth indefinitely. Our simulations have shown this behavior to disrupt seriously the electron beam, as might be expected.

Image charge flow can be described reasonably well by the wave equation

$$\frac{\partial^2 \rho}{\partial t^2} - v_H^2 \frac{\partial^2 \rho}{\partial z^2} = 0 \quad , \quad (2)$$

with the boundary conditions $\rho + \rho_0 = 0$ at either end, $z = 0$ and L . Here, ρ and ρ_0 are the charge per unit length on the helix and in the beam. Eq. (2) can be solved to give a recurrence relation for, e.g., charge flowing to the right at the right boundary.

$$\rho_+(t, L) = \rho_+(t - 2L/v_H, L) - \rho_0(t - L/v_H) - \rho_0(t - 2L/v_H - L/v_B) \quad (3)$$

Beam charge is parameterized by the time it entered the helix at the left.

The asymptotic solution to Eq. (3) is

$$\begin{aligned} \rho_+(\omega = 0) &= -\rho_0 (1 + v_H/v_B)/2 \quad , \\ \rho_+(\omega = \pi v_H/nL) &= -\rho_0 (2/n\pi) \omega \tau / (1 + \omega^2 \tau^2) \quad , \end{aligned} \quad (4)$$

for $\omega \tau \gg 1$, where τ is the characteristic rise time of the beam. Our goal, clearly, is to minimize the oscillatory part of ρ_+ . For the example cited above, a helix length of one meter, and $\tau = 80$ ns, the oscillatory part is of order 5%. Additional reduction of transients can be achieved by placing

resistive materials at various points in the system. With a graded resistance between the helix and the outer conductor near the downstream end of the helix, we have reduced transients in simulations to about 1% with $\omega_1\tau \sim 6$.

Even with oscillations in the helix image charges eliminated, a return current

$$I_H/I_B = -(v_H/v_B)^2 \quad (5)$$

persists. This current perturbs the magnetic guide field by

$$\Delta B_z = 2I_H(1 - \alpha)/(R_H c \tan \psi) \quad , \quad (6)$$

or about 300 g for our example. The return current can be eliminated from the helix by terminating it to ground through a resistive load. Alternatively, ΔB_z can be externally compensated.

III. LINEAR THEORY

The helix supports a wave, $\omega = kc \sin \psi$, which interacts with the slow cyclotron wave of the beam, $\omega = kv_B - \omega_c/\gamma$ to produce a convective instability with group velocity approximately $c/2$. The point of intersection of the two waves in $\omega - k$ space is

$$k = \omega_c/\gamma(v_B - c \sin \psi) \quad . \quad (7)$$

Austin Research Associates, Inc. has obtained an approximate analytic growth rate for a radially homogeneous beam, $\gamma \gg 1$, $kR_B \gg 1$, $R_H = R_B$, and $R_W = \infty$.⁶ The latter two constraints can be relaxed to give

$$\Gamma = \frac{\omega_p}{2\gamma} \left(\frac{\Omega_c R_B}{c} \sin 2\psi \right)^{1/2} \left(e^{-2k(R_H - R_B)} - e^{-2k(R_W - R_B)} \right) \quad . \quad (8)$$

To improve upon these estimates, we employ GRADR, a computer code which solves Maxwell's equations together with the

relativistic cold fluid equations linearized about any given cylindrical beam equilibrium.⁴ In particular, it can treat the effects of beam energy radial inhomogeneity, $\gamma(r)$, caused by the self-fields of the beam. Fig. 2 presents results from this code for the parameters used throughout this article.

The growth rate peaks at $\Gamma = 6.8 \cdot 10^8 \text{ sec}^{-1}$, corresponding to $k = 0.46 \text{ cm}^{-1}$ and $\omega = 3.7 \cdot 10^9 \text{ sec}^{-1}$. With a computed group velocity of 0.6 c, the instability growth length is 27 cm, or about two wavelengths. Incidentally, Eq. (7) predicts the numerically determined wavenumber precisely, if we use for γ its value at the beam edge, 5.75. With the same choice, Eq. (8) gives a growth rate too large by nearly a factor of two. In view of the many approximations required in obtaining Eq. (8), agreement is good.

IV. WAVE GROWTH AND SATURATION

In order to corroborate linear theory and, more importantly, to determine the saturation level and mechanism for the beam-helix cyclotron instability, we carried out a series of two-dimensional, relativistic, electromagnetic computer simulations with CCUBE⁵ configured for cylindrical coordinates. Simulations employed the beam and guide field parameters previously described but varies lengths and radii for the helix and outer conductor. Numerically well matched end conditions were used for the helix, rather than the physical terminations shown in Fig. 1, because we were interested primarily in wave growth and saturation under ideal conditions. Cyclotron waves were injected at an amplitude of 1/2% of the beam radius at the upstream end of the simulation grid and allowed to grow as they propagated downstream.

For values of R_H in the range 3.2 cm to 4.4 cm, cyclotron waves grew spatially (as measured by modulation of the beam radius and by field strengths at the helix) with a growth length approximating that predicted by GRADR until either beam particles struck the helix or waves left the downstream end of the grid. Well depth increased approximately logarithmically with modulation amplitude.⁷ We expect that saturation by particle trapping would occur for sufficiently large helix radius; however, cost and time constraints prevent pursuing this issue.

These simulations suggest that helix and conductor radii of 3.8 cm and 5.7 cm will prove suitable for the planned experiment, and so we have used those values throughout the report in numerical examples. With these radii the beam wave strikes the helix after about 4.5 e-foldings, or 120 cm. The helix should, therefore, be terminated at 100 cm, giving a potential well depth of 0.5 MeV. Maximum acceleration field strength on axis is 120 keV/cm, which is more than adequate. Corresponding electric field strength at the helix is about 1/3 that amount and should not cause breakdown problems.

Fig. 3 shows wave growth and saturation in a 160 cm system.

V. WAVE EXTRACTION

Fig. 4 contrasts the radial structure of characteristic components of the linearized cyclotron eigenmode, determined by GRADR, in the helix and in a metal cylinder of equal radius. Frequency and wavenumber correspond to the maximum growth rate from Fig. 2, and, with frequency fixed, wavenumber is essentially identical for the two geometries. If the disparity in radial structure persists in the nonlinear regime,

as is likely, a real danger exists that wave coherence may be lost when the cyclotron waves exit the helix amplifier. In a few months, we hope to begin simulation studies of adiabatic transitions designed to minimize any such ill effects.

VI. ACKNOWLEDGMENT

We are indebted to E. P. Cornet for his valuable comments at various stages of this research.

REFERENCES

*Research supported jointly by the Air Force Office of Scientific Research and the Energy Research and Development Administration.

1. See, e.g., papers from the 1977 Particle Accelerator Conference (Chicago, 16-18 Mar. 77), *IEEE Nuc. Sci.* 24, 1625-1667 (1977).
2. M. L. Sloan and W. E. Drummond, *Phys. Rev. Lett.* 31, 1234 (1973).
3. W. E. Drummond, et al., unpublished.
4. B. B. Godfrey, in preparation.
5. B. B. Godfrey and W. R. Shanahan, in N. G. Cooper (ed.), "Theoretical Division Annual Report, July 1975-Sept. 1976," LA-6816-PR (Los Alamos Scientific Laboratory, 1977), p. 147.
6. W. E. Drummond, et al., AFWL-TR-75-296 (Air Force Weapons Laboratory, Albuquerque, 1976), App. O.
7. B. B. Godfrey, *IEEE Plas. Sci.*, to be published.

CAPTIONS

Figure 1. Conceptualized transition from cylindrical waveguide to helical amplifier cavity. Radial dimensions are scaled to $R_B = 2.65$ cm, $R_H = 3.8$ cm, and $R_W = 5.7$ cm. Small plus signs represent image charges.

Figure 2. Frequency and growth rate of the beam-helix cyclotron instability for a 15° helix pitch as a function of wavenumber. Units are ω_p and ω_p/c , respectively.

Figure 3. Growth of cyclotron wave in helical cavity. Plots, top to bottom, are electron positions in cavity cross section, contours of the electrostatic potential, and electron axial momenta. Helix is at $r = 3.8 c/\omega_p$.

Figure 4. Plots of perturbed radial momentum and axial electric field of a slow cyclotron wave in a 15° helix or in a waveguide each of radius $3.8 c/\omega_p$.

HELIX UPSTREAM TERMINATION

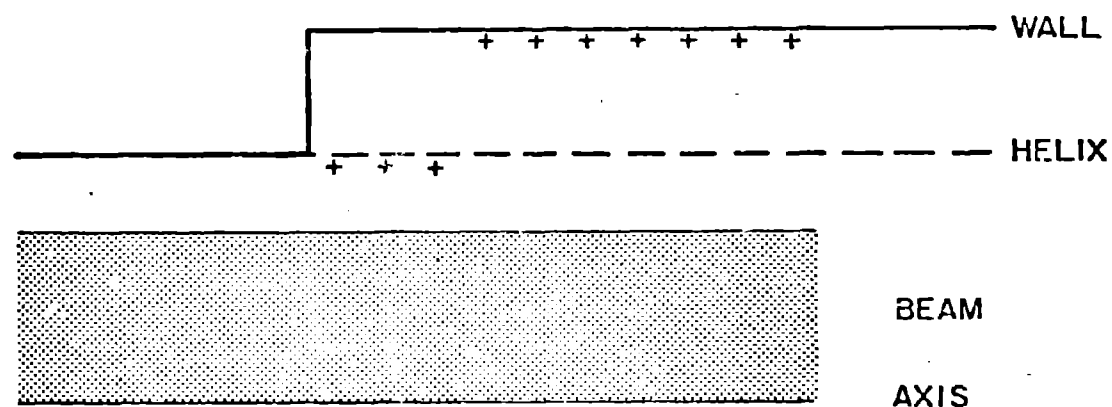


Fig. 1

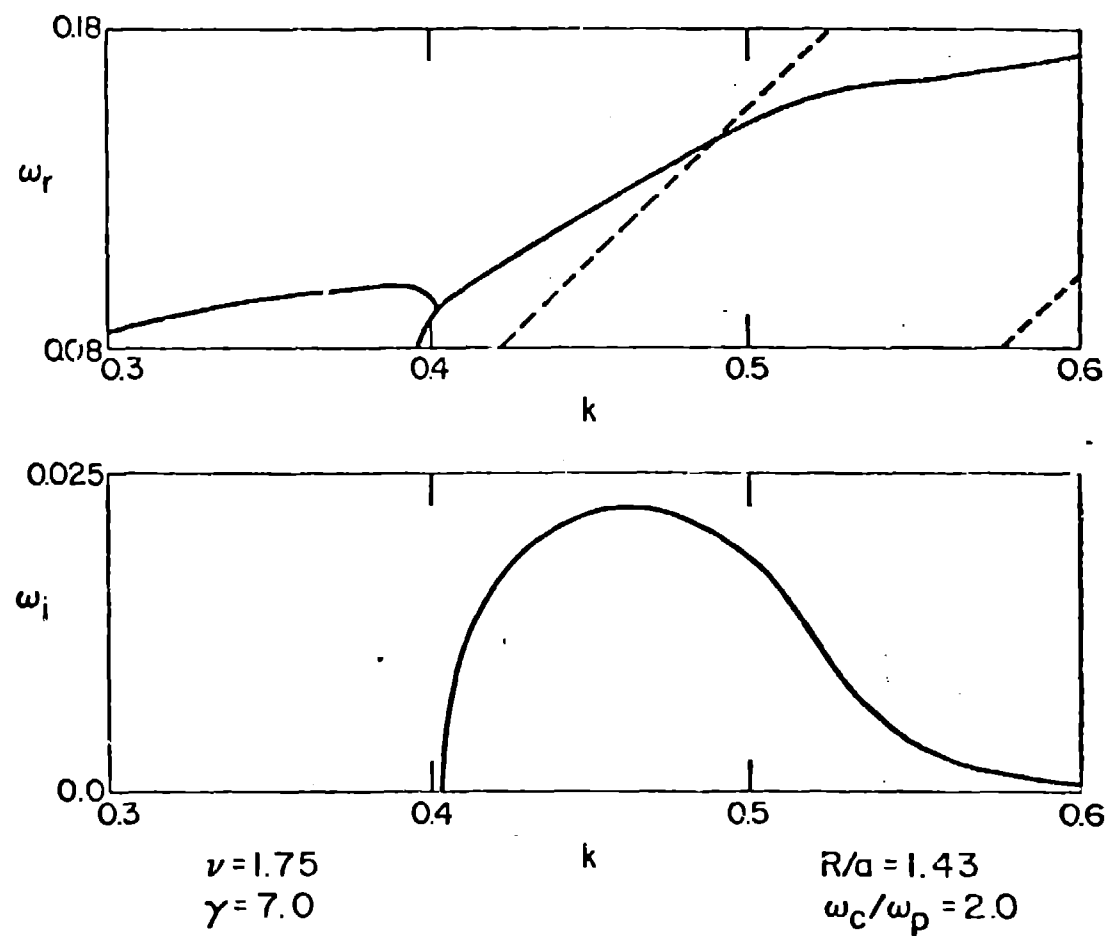


Fig. 2

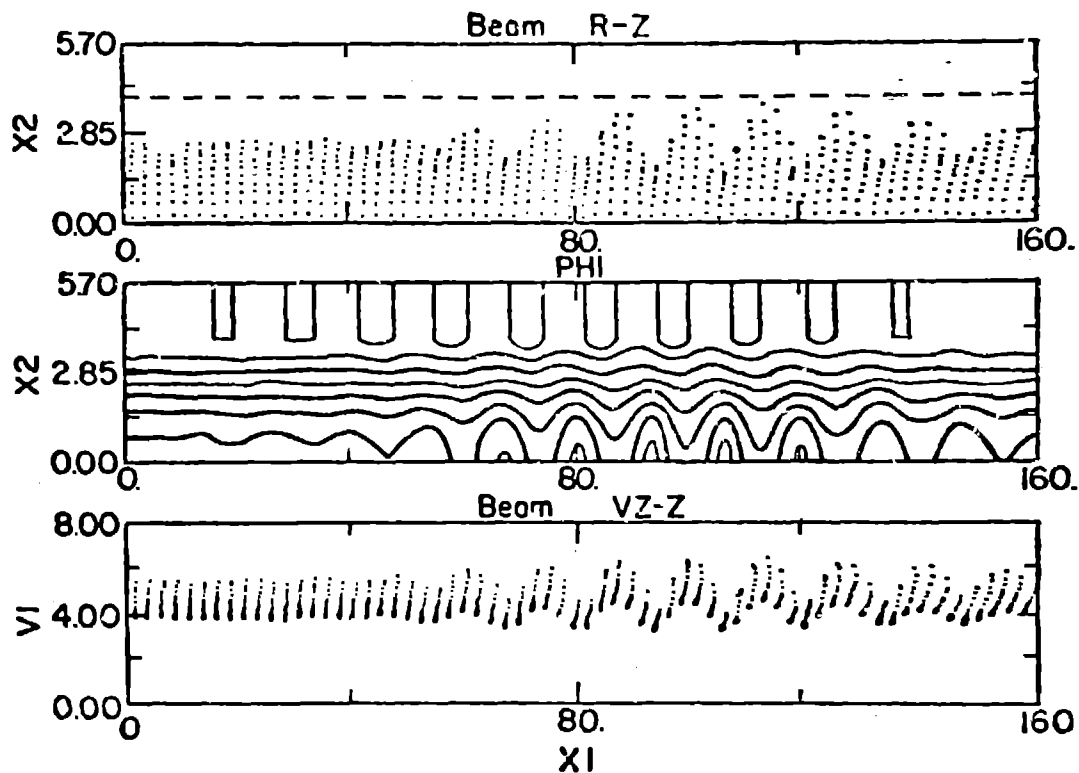


Fig. 3

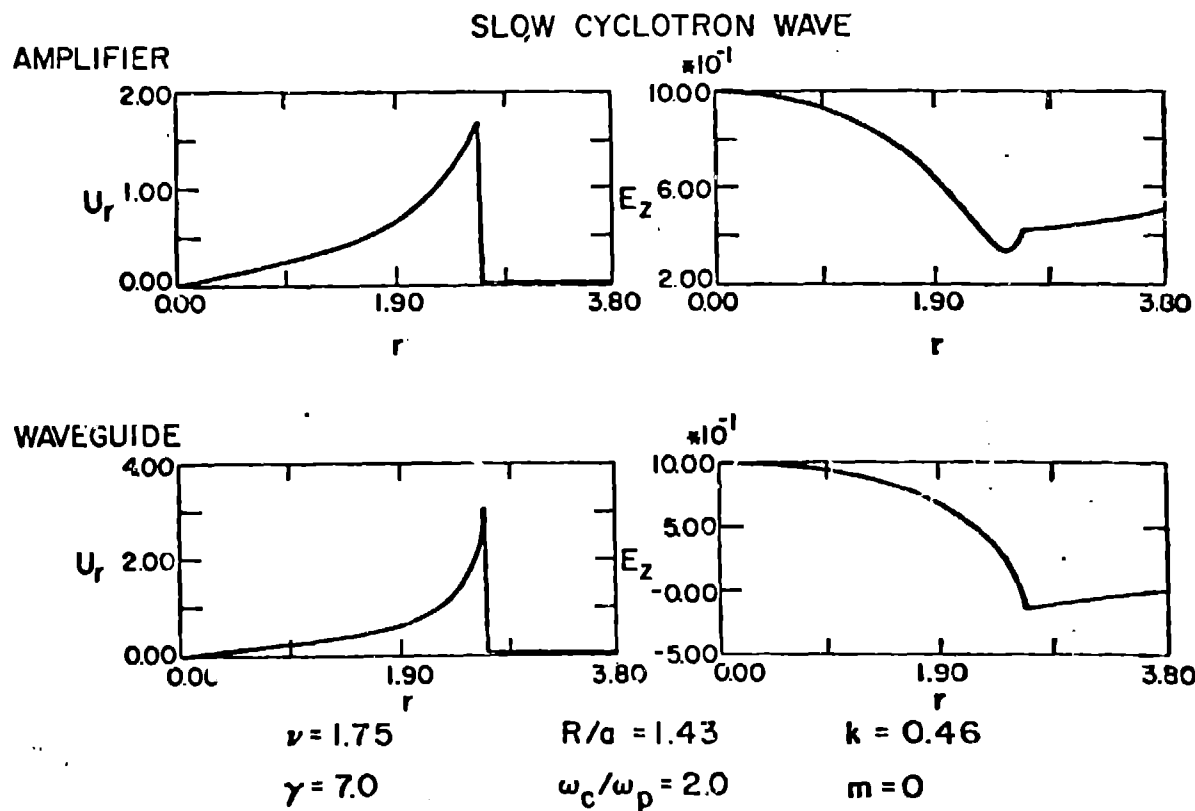


Fig. 4